APPLIED MECHANICS

The results of kinematic and force analysis of the new six-link converting mechanism of the sucker rod pumper drive (SRPD) are presented in this paper and the advantages of the alternative design are substantiated. Using a straight-line generating mechanism allows reducing essentially converting mechanism dimensions and metal consumption as compared with traditionally used SRPD with swinging balancer and crank-based counterweight, first of all, due to eliminating the complicated arc head (so-called «horse-head») of the existing units. However, in order to make sure the working capacities of non-balancer mechanism, kinematic and force characteristics have to be studied. The results of mathematical modeling of the six-link mechanism confirm the qualitative advantages of the straight-line generator. As a result of the study of the rectilinear-guiding mechanism as a transforming mechanism for the drive of sucker rod pumping units, the laws of motion of the links, position, speed and acceleration of all points were determined. To solve the problem of kinematic analysis, the method of closed vector contours was used, which makes it possible to determine the functions of the position of links and analogs of speeds and accelerations. When solving the problem of strength analysis, the equilibrium of each link was considered. As a result of force analysis, jointly solving the equilibrium equations of the links of the six-link hinge-lever mechanism, the reactions of the hinges of the mechanism are determined. A computer model for studying the kinematics and kinetostatics of the converting mechanism of the sucker rod pumping unit drive has been developed

Keywords: sucker rod pumper drive, converting mechanism, straight-line generator, crank, balancer, kinematic analysis, force analysis

UDC 622. 276
DOI: 10.15587/1729-4061.2020.218551

KINEMATIC AND KINETOSTATIC ANALYSIS OF THE SIX-LINK STRAIGHT-LINE GENERATING CONVERTING MECHANISM OF THE UNBALANCED SUCKER ROD PUMPER DRIVE

Rakhmatulina Ayaulym
PhD*
Department of Engineering Graphics and Applied Mechanics
Almaty Technological University
Tole bi str., 100, Almaty, Kazakhstan, 050012
E-mail: kazrah@mail.ru
Ibrayev Sayat
Doctor of Engineering*
E-mail: sayat_m.ibrayev@mail.ru
Imanbayeva Nurbibi
PhD*
E-mail: imanbaevan@mail.ru
Ibrayeva Arman
Postgraduate Student
Department of Mechanics**
E-mail: sayatqyzy@gmail.com
Tolebayev Nurzhan
Postgraduate Student**
E-mail: nur-tul@mail.ru
*Department of Mechanical Engineering and Robotics
Institute of Mechanics and Engineering Science
named after acad. W. A. Dzholdasbekov
Kurmangazy str., 29, Almaty, Kazakhstan, 050000
**Al-Farabi Kazakh National University
Al-Farabi ave., 71, Almaty, Kazakhstan, 050040

Received date 02.11.2020
Accepted date 09.12.2020
Published date 16.12.2020

1. Introduction

In the context of drop in world prices for petroleum products, the issue of reducing the cost of oil production is of particular relevance. The improvement of mechanisms and machines for the oil and gas industry is associated with the search for alternative approaches to traditional methods, with the study of new functional capabilities of mechanisms in modern technology using modern methods for mathematical modeling and optimal design.

The main purpose of the executive mechanism of the rocking machine is to convert the uniform rotation of the crank into the reciprocating movement of the plunger [1–5]. The most common type of drive for sucker rod pumping units

all over the world is mechanical drives balanced individually. The alternative design based on a straight-line generating mechanism is proposed, which allows eliminating the arc head (so-called «horse-head») of the existing devices, having a complex structure, and additional flexible links, leading to a simplified design. However, in order to make sure the working capacities, kinematic and force characteristics of the mechanism have to be studied.

Thus, the works devoted to the study of the possibility of using a rectilinear guide mechanism as a converting mechanism for the drive of sucker rod pumping units are of scientific importance.

2. Literature review and problem statement

In [1], the results of research are given, a mathematical dynamic model of a real sucker rod pump is developed based on the identification of methods using measurements of input-output data. Tests were carried out in a real plant to check the validation and robustness of the controller algorithm used. The results are also compared with a conventional PID controller. We also applied modeling and identification tools as well as a robust adaptive controller (called IVS-MRAC) to an oil well sucker rod system. It should be noted that one of the main problems that has been repeatedly discovered is the verification of models (mainly using material balance, energy, etc.) for these systems. Because the pumping components such as the rod string and the downhole pump are located deep within and without easy access, the system is fully instrumented and the bottom is accessible and visible. The results also show that the adaptive controller can satisfactorily manage the fluid level in the annular well despite the presence of model uncertainties, variation parameter and disturbance. Moreover, the results show that the management method can increase productivity and reduce maintenance costs.

However, in [1], only the dynamic model of a real rod pump is considered and the load on the links of the converting mechanism of rod pumping units and the load at the links point of the rod column are not taken into account.

In [2], a method for solving a one-dimensional wave equation is considered, which describes the longitudinal vibrations of a sucker rod string. Depending on the boundary conditions, the application of the equation includes diagnostic analysis to calculate pump displacements and forces based on surface measurements and prediction, analysis to calculate surface forces based on polished surface of rod movement and pump force. Experimental verification of the model is also performed.

However, the effect of longitudinal vibrations of the pump rod column on the movement of the links point of the rod column is not considered here. The suspension point of the column of the rods of the converting mechanism of rod pumping units should make a straight line movement that approaches the ideal straight line.

The work [3] proposes a design of an oil pumping unit that has an original structure and provides the following advantages over other types of oil production equipment:

– it consumes about 1.5–1.7 times less electricity than conventional sucker rod pumps;

– increases the service life of the gearbox due to the absence of negative torque on the output shaft;

– does not require a solid and high foundation.

In the proposed design of the oil pumping unit in [3], flexible links are used that are sensitive to vibrations of the elements of the pumping unit.

In [4], a dynamic analysis of the pumping system mechanism used for deep oil production is proposed. Dynamic analysis includes the determination of kinematic and dynamic parameters that characterize the vibrations of the pumping mechanism elements of the unit. The law of variation of the generalized coordinate of the mechanism has an experimentally defined form. Kinematic models were developed for longitudinal and transverse vibrations of the links, which were processed by a computer and led to the laws of time variation of longitudinal and transverse vibrational displacements, respectively, speed and acceleration, which determine the system of vibrational motion. These laws have been tested and confirmed by experimental research.

In [5], a model of the «Horse Head» sucker rod was developed. This model is 88 cm long, 52 cm wide and 56.5 cm high.

This practical model has the following limitations:

– apart from the analog counter, there was no computer or electronic monitoring system for recording experimental data, since the main goal of the authors was to create an inexpensive experimental model;

– in the second phase of the experiment, water production was relatively high compared to oil production. One limitation of the model that may have contributed to this is that the casing model was perforated very close to the base of the reservoir model, i. e. the water-bearing zone. Uniform casing perforation within the pay zone will increase oil production.

A complete kinematic and force analysis was not performed for the developed practical model. The design is justified by experimental approximate calculations.

In [6], the tasks of the research are the development of a telescopic sliding structure of the balancer with an electric motor and an automatic remote control system, the development of an improved design of the ladder of the ground drive of the sucker rod pumping unit. The technical result of improving the design of the sucker rod pumping unit balancer drive is to automate the process of preparing the sucker rod pumping unit drive for planned and overhaul repairs, as well as reducing the time spent on preparatory work for well workover due to the use of the balancer arm in the design of the device, made in the form of a telescopic structure with the possibility of longitudinal movement equipped with an electric motor. An additional result is an increase in the safety of repair and installation work by eliminating the need for manual partial maintenance and dismantling the balancer head.

In [7], a recurrent neural network is considered, which can assume a malfunction of the rod pumping system by predicting future model parameters of the mathematical formulation of the dynamometer card. In this example, a guess can be made 16.7 hours before the problem occurs.

In [8], exemplary embodiments of systems and methods for controlling the stroke of a sucker rod pump unit for controlling the flow of fluid are given. Here the scope of the invention relates generally to the control of rod pumping units, and more particularly to methods and system for controlling the rod pumping unit for increasing the fluid flow induced by the rod pumping unit.

Another drawback is related to increased gearbox wear, due to the periodical impact loads in the gearbox axe [9]. Optimal balancing of the traditional converting mechanisms with two-arm balancer and rotary balancing is carried out in the latter publication, a methodology and software package

of applied programs for kinematic and force analysis were created. The developed technique and programs were applied to calculate rocking machines sucker rod pumping units of type SRPD 6-2.5-3500 and SRPD 8-3-4500 of AZTM factory (Almaty, Kazakhstan) with maximum loads in the wellhead gland of 6 t and 8 t [10], static load values by going up and down are: P_U=80 kN, P_D=53 kN.

The main reason for the mentioned drawbacks is poor balancing of the device, resulting in big loads on the crank finger and alternating sign of this load (tangential component of crank reaction). Increased wear of the elements and frequent damage of the gearbox are the reason for applying expensive Novikov-type gearboxes. While desiring to increase the rod stroke by increasing the crank length, the mechanism operates in unfavorable modes of force transmission: poor angles of motion and force transmission lead to big joint reactions.

For instance, Watt mechanisms are not suitable because the straight-line segment of the coupler curve lies between two fixed joints on the frame-axes. Thus, the mechanism does not allow access to the outfall of the well, while in the existing rocking machine the access to the outfall is provided simply by the lateral tilt of the arc-head. For the same reason, the mechanisms of Robert and Grashof are found to be unsuitable as well. Chebyshev straight-line mechanism is found to have large relative dimensions in comparison with the length of the straight-line segment of the coupler curve, while the mechanisms of Hart and Peaucellier-Lipkin are too complicated and have a large number of links and moveable joints. The result of a preliminary analysis of the functionality of the existing straight-line generators shows that the most appropriate scheme is the four-bar mechanism of Evans. With the additional input dyad group (two links with one internal and two external rotary joints), the six-link linkage is able to transform the rotary motion of the crank to straight-line and reciprocating motion of the end-effector, where the rods column will be hanged.

At the same time, these qualitative advantages have never been confirmed by numerical data, which is the aim of this study.

3. The aim and objectives of the study

The aim of the work is to investigate the possibility of using a six-link rectilinear guide mechanism as a converting mechanism for the drive of sucker rod pumping units and to create a mathematical model for calculating parameters.

To achieve the aim, the following objectives were set:

– to derive basic equations for the kinematic analysis of the six-link mechanism and determine the laws of motion of all moveable links, to carry out position, speed and acceleration analysis of all mechanism joints;

– to determine reactions in the mechanism joints as a result of force analysis.

4. Methods and data

To achieve the research goal, we used methods for solving problems in theoretical mechanics, the theory of machine mechanisms, and numerical methods. In solving the problem of kinematic analysis, we use the vector closed loop method.

The converting mechanism of the rocking machine shown in Fig. 1 is a mechanism of the II class, which consists of a crank (1), a double-drive group (2, 3) FCO, also attached double-drive group (4, 5) ABC. The working point is the point *D* of the rod string.

The purpose of the kinematic analysis is to determine the trajectories of the point *D* of the rod string suspension at uniform rotations of the crank GF, as well as to determine the speeds and acceleration of this point.

It is considered that the law of change in the angular position of the crank 1 is given according to the law $\varphi=\varphi_0+\omega t$, where ω=const is the constant angular velocity of crank rotation. For the analysis of the positions, it is assumed that *N* of the finitely distant angular positions of the crank φ_i is given by the formula, where $i=1,..,N$,

$$\varphi_i = 2\pi\frac{i-1}{N-1}. \quad (1)$$

With these laws of change in the angular positions of the crank, it is necessary to determine the angular positions of all links by means of sequential kinematic analysis of class II two-flood groups. First, consider the vector contour GFO (Fig. 2).

Let us compose the equation of closedness of the vector contour:

$$\vec{l}_1+\vec{S}=\overrightarrow{l_{OG}}. \quad (2)$$

We project the vectors of equation (2) on the coordinate axis and have:

$$l_1\cos\varphi_1 - S\cos(2\pi-\varphi_S) = -l_{OG}\cos\gamma, \quad (3)$$

$$l_1\sin\varphi_1 + S\sin(2\pi-\varphi_S) = l_{OG}\sin\gamma. \quad (4)$$

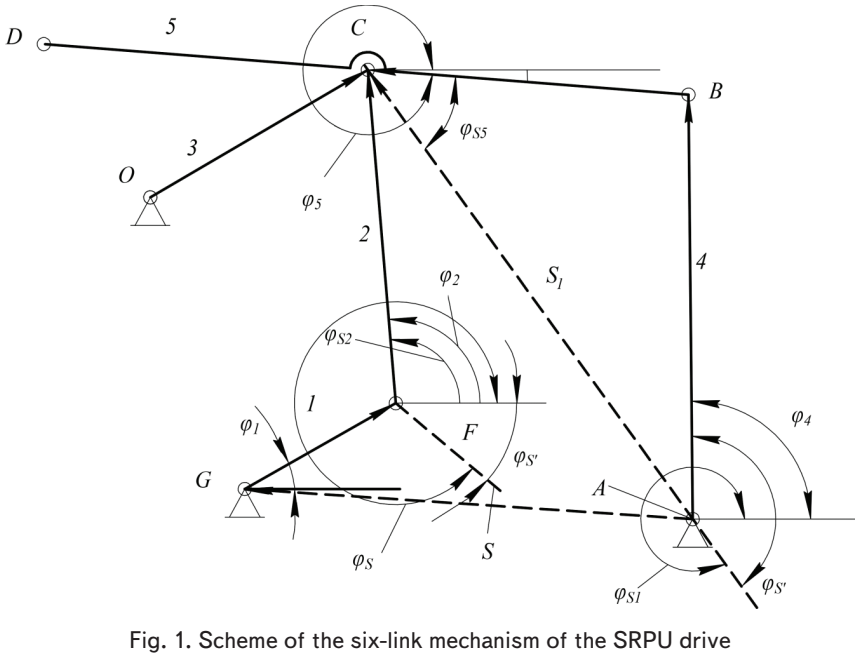

Fig. 1. Scheme of the six-link mechanism of the SRPU drive

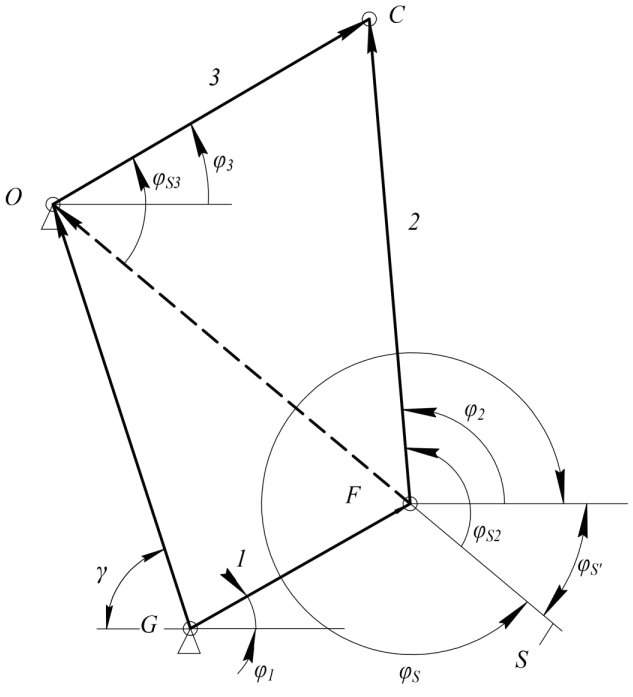

Fig. 2. To the kinematic analysis of the OCF two-runner group γ

Considering $\cos(2\pi-\varphi_s)=\cos\varphi_s$ and $\sin(2\pi-\varphi_s)=-\sin\varphi_s$ from equations (3) and (4) we obtain:

$$\operatorname{tg}\varphi_S=\frac{l_1\cos\varphi_1-l_{OG}\cos\gamma}{l_1\sin\varphi_1+l_{OG}\cos\gamma}. \tag{5}$$

The quarter of the trigonometric circle, in which the angle S is located, is completely determined by the sign of the numerator and denominator of expression (5). Further, from equation (3) we determine the modulus of the vector S:

$$\vec{S}=\frac{l_1\cos\varphi_1-l_{OG}\cos\gamma}{\cos\varphi_S}. \tag{6}$$

Next, we consider (Fig. 2) the *OCF* triangle. The angles of inclination of the vectors l_2 and l_3 to the vector S are denoted by φ_{S2} and φ_{S3}, respectively.

We then have the following two equations:

$$l_2^2=l_3^2+S^2-2l_3S\cos\varphi_{S3}, \tag{7}$$

$$l_3^2=l_2^2+S^2+2l_2S\cos\varphi_{S2}. \tag{8}$$

From equations (7) and (8), we determine the angles:

$$\varphi_{S3}=\arccos\frac{l_3^2+S^2-l_2^2}{2l_3S}, \tag{9}$$

$$\varphi_{S2}=\arccos\frac{l_3^2-S^2-l_2^2}{2l_2S}. \tag{10}$$

Next, we find the angles, that is, the functions of the positions of links 2 and 3:

$$\varphi_2=\varphi_{S2}+\varphi_S,$$

$$\varphi_3=\varphi_{S3}+\varphi_S. \tag{11}$$

Next, we compose the vector equation of the closed-form of the *AGFC* contour (Fig. 1). We have:

$$\vec{l}_{GA}+\vec{l}_1+\vec{l}_2=\vec{S}_1. \tag{12}$$

The equations of the projections of the vectors of this equation on the *Ox* and *Oy* axes will be:

$$\begin{cases}-l_{GA}^x+l_1\cos\varphi_1-l_2\cos\varphi_2'=-S_1\cos\varphi_{S1}',\\ l_{GA}^y+l_1\sin\varphi_1+l_2\sin\varphi_2'=S_1\sin\varphi_{S1}'.\end{cases} \tag{13}$$

From (Fig. 2) determine the angles:

$$\varphi_2'=\pi-\varphi_2,$$

$$\varphi_{S1}'=2\pi-\varphi_{S1}, \tag{14}$$

then, given (14), the expression (13) will take the following form:

$$\begin{cases}-l_{GA}^x+l_1\cos\varphi_1+l_2\cos\varphi_2=-S_1\cos\varphi_{S1},\\ l_{GA}^y+l_1\sin\varphi_1+l_2\sin\varphi_2=-S_1\sin\varphi_{S1}.\end{cases} \tag{15}$$

From where we find:

$$\varphi_{S1}=\operatorname{arctg}\left(\frac{-l_{GA}^y-l_1\sin\varphi_1-l_2\sin\varphi_2}{l_{GA}^x-l_1\cos\varphi_1+l_2\cos\varphi_2}\right) \tag{16}$$

and

$$S_1=\frac{l_{GA}^x-l_1\cos\varphi_1-l_2\cos\varphi_2}{\cos\varphi_{S1}}. \tag{17}$$

Now we consider the triangle *ACB* and get:

$$l_4^2=l_5^2+S_1^2-2l_5S_1\cos(\varphi_{S15}), \tag{18}$$

$$l_5^2=l_4^2+S_1^2-2l_4S_1\cos(\varphi_{14}). \tag{19}$$

Then from equations (18), (19) we find expressions for the angles:

$$\varphi_{S15}=\arccos\left(\frac{l_5^2+S_1^2-l_4^2}{2l_5S_1}\right), \tag{20}$$

$$\varphi_{S14}=\arccos\left(\frac{l_5^2+S_1^2-l_4^2}{2l_4S_1}\right). \tag{21}$$

Next, we find the angles:

$$\varphi_5=\varphi_{S1}+\varphi_{S15}, \tag{22}$$

$$\varphi_4=\varphi_{S1}+\varphi_{S14}. \tag{23}$$

The Maple system was used for mathematical modeling of kinematic calculations.

After determining the angular positions of the links of the conversion mechanism of the rocking machine, we can determine the absolute coordinates of all points of all links. Using the found absolute coordinates of all hinges and the operating point *D*, it is possible to construct an animation of the movement of the SRPU drive converter mechanism (Fig. 3, *a*, *b*).

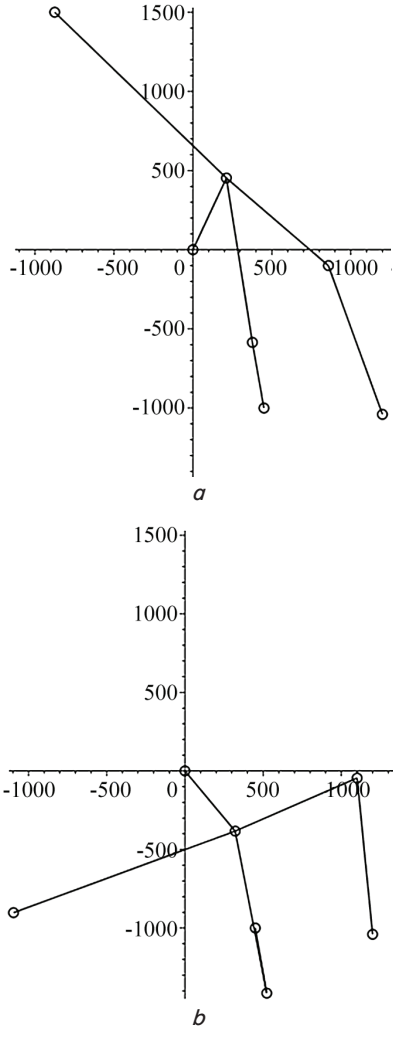

Fig. 3. Movement of the SRPU drive converter mechanism: *a* – upper mechanism position; *b* – lower mechanism position

Further, to determine the speeds and accelerations of the links of the mechanism, we compose the vector equation of the closed-form of the *GFCO* contour (Fig. 1).

$$\vec{l}_{OG}+\vec{l}_3+\vec{l}_2=\vec{l}_1. \tag{24}$$

Projecting this equation on the O_x and O_y axes, we obtain:

$$-l_{OG}^x+l_3\cos\varphi_3-l_2\cos\varphi_2=l_1\cos\varphi_1, \tag{25}$$

$$l_{OG}^y+l_3\sin\varphi_3-l_2\sin\varphi_2=l_1\sin\varphi_1. \tag{26}$$

To determine the analogs of the angular velocities ω_2 and ω_3 of links 2 and 3, we differentiate equations (25) and (26) with respect to the generalized coordinate φ_1. Let us introduce the notation $d\varphi_3/d\varphi_1=U_{31}$; $d\varphi_2/d\varphi_1=U_{21}$.

Then:

$$-U_{31}l_3\sin\varphi_3+U_{21}l_2\sin\varphi_2=-l_1\sin\varphi_1, \tag{27}$$

$$U_{31}l_3\cos\varphi_3+U_{21}l_2\cos\varphi_2=-l_1\cos\varphi_1. \tag{28}$$

From the angles included in equation (27), we subtract the total angle φ_3, which corresponds to the rotation of the coordinate axes *xOy* (Fig. 1) by the total angle φ_3. We have:

$$U_{21}l_2\sin(\varphi_2-\varphi_3)=-l_1\sin(\varphi_1-\varphi_3). \tag{29}$$

Whence we get the expression for the analogue U_{21} of the angular velocity ω_2:

$$U_{21}=-\frac{l_1\sin(\varphi_1-\varphi_3)}{l_2\sin(\varphi_2-\varphi_3)}. \tag{30}$$

After a similar transformation of the same equation by rotating the coordinate axes by an angle φ_2, we obtain an expression for the analogue U_{31} of the angular velocity ω_2:

$$U_{31}=-\frac{l_1\sin(\varphi_1-\varphi_2)}{l_3\sin(\varphi_3-\varphi_2)}. \tag{31}$$

Now we consider the vector contour AGFCB. Let us compose the equation of closedness of the vector contour:

$$\vec{l}_{AG}+\vec{l}_1+\vec{l}_2=\vec{l}_4+\vec{l}_5. \tag{32}$$

We project the vectors of equation (32) on the coordinate axis and have:

$$-l_{AG}^x+l_1\cos\varphi_1+l_2\cos\varphi_2=l_4\cos\varphi_4+l_5\cos\varphi_5, \tag{33}$$

$$l_{AG}^y+l_1\sin\varphi_1+l_2\sin\varphi_2=l_4\sin\varphi_4+l_5\sin\varphi_5. \tag{34}$$

To determine the analogs of the angular velocities ω_4 and ω_5 of links 4 and 5, we differentiate equations (33) and (34) with respect to the generalized coordinate φ_1. Let us introduce the notation:

$$\frac{d\varphi_2}{d\varphi_1}=U_{21},\ \frac{d\varphi_4}{d\varphi_1}=U_{41},\ \frac{d\varphi_5}{d\varphi_1}=U_{51}.$$

Then:

$$-l_1\sin\varphi_1-U_{21}l_2\sin\varphi_2=-U_{41}l_4\sin\varphi_4-U_{51}l_5\sin\varphi_5, \tag{35}$$

$$l_1\cos\varphi_1+U_{21}l_2\cos\varphi_2=U_{41}l_4\cos\varphi_4+U_{51}l_5\cos\varphi_5. \tag{36}$$

Let us write equation (36) in vector form:

$$\vec{l}_1+U_{21}\vec{l}_2=U_{41}\vec{l}_4+U_{51}\vec{l}_5. \tag{37}$$

Equation (37) multiplying by the rotation matrix, that is, turning all vectors by a common angle φ_5 we have:

$$l_1\sin(\varphi_1-\varphi_5)-U_{21}l_2\sin(\varphi_2-\varphi_5)=U_{41}l_4\sin(\varphi_4-\varphi_5). \tag{38}$$

Whence we get the expression for the analogue U_{41} of the angular velocity ω_4:

$$U_{41}=-\frac{l_1\sin(\varphi_1-\varphi_5)+U_{21}l_2\sin(\varphi_2-\varphi_5)}{l_4\sin(\varphi_4-\varphi_5)}. \tag{39}$$

After a similar transformation of the same equation by rotating the coordinate axes by an angle φ_4, we obtain an expression for the analogue U_{51} of the angular velocity ω_5:

$$U_{51}=-\frac{l_1\sin(\varphi_1-\varphi_4)+U_{21}l_2\sin(\varphi_2-\varphi_4)}{l_5\sin(\varphi_5-\varphi_4)}. \tag{40}$$

We also find analogs of the velocities U_{21} and U_{31}, U_{41} and U_{51} of the angular velocities ω_2 and ω_3, ω_4 and ω_5. Then we determine the linear velocities of all points of the SRPU drive mechanism.

We determine the angular velocities ω_2 and ω_3, ω_4 and ω_5:

$$\omega_2 = \omega_1 \cdot U_{21},$$

$$\omega_3 = \omega_1 \cdot U_{31},$$

$$\omega_4 = \omega_1 \cdot U_{41},$$

$$\omega_5 = \omega_1 \cdot U_{51}. \quad (41)$$

Then the values of the velocity projections on the coordinate axes of the point D of the suspension of the column of rods are determined as follows:

$$\begin{cases} V_D^x = V_A^x - l_4\omega_4 \sin\varphi_4 - l_5\omega_5 \sin\varphi_5, \\ V_D^y = V_A^y - l_4\omega_4 \cos\varphi_4 - l_5\omega_5 \cos\varphi_5. \end{cases} \quad (42)$$

The acceleration points D of the suspension of the column of rods of the considered SRPU drive mechanism are also determined in the same way.

On the basis of the obtained expressions, a computer model of the kinematic analysis of the six-link rectilinear-guiding converting mechanism of the SRPU drive was developed.

Next, we will conduct a kinetostatic analysis of the six-link mechanism of the SRPU drive. The mechanism is affected by the load in the wellhead gland and gravity of the links and weights (Fig. 4). We do not take into account friction forces in the joints and inertia forces, since the values of these forces are insignificant.

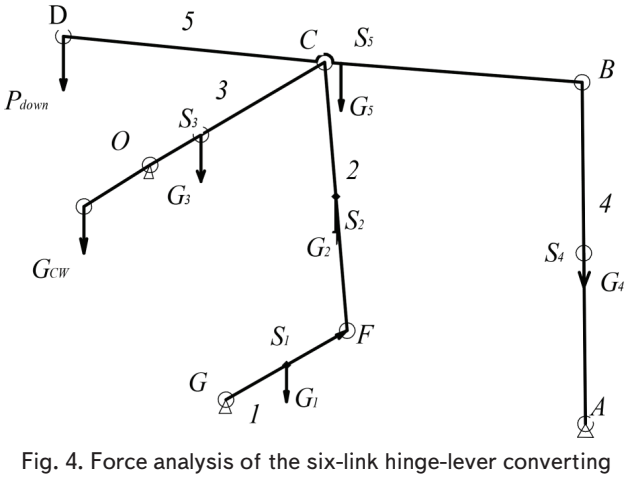

Fig. 4. Force analysis of the six-link hinge-lever converting mechanism of rocking machines

We consider the balance of each link. The crank is acted upon at point S_1 in the center of mass of the crank $F_1 = G_1 - m_1 a_{S1}$, the force and engine torque M_D also at point F the reaction R_{21} and at point G the reaction R_{01}, where a_{S1} is acceleration in the center of mass link GF. We compose the equilibrium equations for the 1st link:

$$R_{01}^x + R_{21}^x = 0,$$

$$-F_1 + R_{01}^y + R_{21}^y = 0,$$

$$F_1(X_{S1} - X_A) + R_{21}^y(X_F - X_G) + R_{21}^x(Y_F - Y_G) + M_D = 0. \quad (43)$$

Now we consider the balance of the 2nd link, the connecting rod. The connecting rod is acted upon in the center of mass of the connecting rod $F_2 = G_2 - m_2 a_{S2}$ – the force and the reaction forces R_{21}, R_{32}, R_{54}, R_{52}, where a_{S2} is acceleration in the center of mass link FC.

Let us compose the equilibrium equations of the connecting rod – 2nd link:

$$-R_{21}^x + R_{32}^x + R_{52}^x = 0,$$

$$-F_2 - R_{21}^y + R_{32}^y + R_{52}^y = 0,$$

$$F_2(X_{S2} - X_F) + R_{32}^y(X_C - X_F) + R_{52}^y(X_C - X_F) + R_{52}^x(Y_F - Y_C) = 0. \quad (44)$$

Now let us consider the equilibrium of the 3rd link. The third link is acted upon at the point S_3 by the force, $F_3 = G_3 - m_3 a_{S3}$ – the force, at the point L by the force G_{CW} – the weight of the counterweight and reaction forces R_{03}, R_{32}, where a_{S3} is acceleration in the center of mass 3rd link.

Then for the 3rd link:

$$R_{04}^x - R_{32}^x = 0,$$

$$-F_3 + R_{03}^y - R_{32}^y - G_{CW} = 0,$$

$$F_3(X_{S3} - X_O) + R_{32}^y(X_C - X_O) + R_{32}^x(Y_O - Y_C) + G_{CW}(X_{CW} - X_O) = 0. \quad (45)$$

Consider the balance of the 4th link, the connecting rod. The connecting rod is acted upon in the center of mass of the connecting rod, $F_4 = G_4 - m_4 a_{S4}$ – the force and the reaction forces R_{04}, R_{54}, where a_{S3} is acceleration in the center of mass 4th link. Then we compose the equilibrium equations of the connecting rod – the 4th link:

$$R_{04}^x + R_{54}^x = 0,$$

$$-F_4 + R_{04}^y + R_{54}^y = 0,$$

$$F_4(X_{S4} - X_A) + R_{54}^y(X_B - X_A) + R_{54}^x(Y_A - Y_B) = 0. \quad (46)$$

The 5th link is acted upon in the center of $F_5 = G_5 - m_5 a_{S5}$ – the force of the fifth link, at the suspension point of the rod string P – the weight of the liquid, the reactive forces R_{54}, R_{52}, where a_{S3} is acceleration in the center of mass 5th link. Then the equilibrium equations of the 5th link:

$$-R_{54}^x - R_{52}^x = 0,$$

$$-G_5 + R_{54}^y + R_{52}^y - P = 0,$$

$$G_5(X_{S5} - X_B) + R_{52}^y(X_C - X_B) + R_{52}^x(Y_B - Y_C) + P(X_D - X_B) = 0. \quad (47)$$

In total, we get a system of 15 equations with 15 unknowns. To solve the equation, a numerical method of Gauss was used in the kinetostatic analysis, and, using the Maple system, a mathematical model of the solution was created.

5. Results

5. 1. Results of the kinematic analysis

As a result of the kinematic analysis, the functions of the positions of the 2, 3, 4 and 5 links were obtained as follows:

$$\varphi_2 = \arccos\frac{l_3^2 - S^2 - l_2^2}{2l_2S} + \operatorname{arctg}\left(\frac{l_1\cos\varphi_1 - l_{OG}\cos\gamma}{l_1\sin\varphi_1 + l_{OG}\sin\gamma}\right), \quad (48)$$

$$\varphi_3 = \arccos\frac{l_3^2 + S^2 - l_2^2}{2l_3S} + \operatorname{arctg}\left(\frac{l_1\cos\varphi_1 - l_{OG}\cos\gamma}{l_1\sin\varphi_1 + l_{OG}\sin\gamma}\right), \quad (49)$$

$$\varphi_4 = \arccos\frac{l_5^2 - S_1^2 - l_4^2}{2l_4S_1} + \\ + \operatorname{arctg}\left(\frac{-l_{GA}^y - l_1\sin\varphi_1 - l_2\sin\varphi_2}{l_{GA}^x - l_1\cos\varphi_1 + l_2\cos\varphi_2}\right), \quad (50)$$

$$\varphi_5 = \arccos\frac{l_5^2 + S_1^2 - l_4^2}{2l_5S_1} + \\ + \operatorname{arctg}\left(\frac{-l_{GA}^y - l_1\sin\varphi_1 - l_2\sin\varphi_2}{l_{GA}^x - l_1\cos\varphi_1 + l_2\cos\varphi_2}\right). \quad (51)$$

Then the absolute coordinates of six-link linkage joints are determined as follows:

$$X_F = X_G + l_1\cos\varphi_1, \quad Y_F = Y_G + l_1\sin\varphi_1, \quad (52)$$

$$X_C = X_G + l_1\cos\varphi_1 + l_2\cos\varphi_2,$$

$$Y_C = Y_G + l_1\sin\varphi_1 + l_2\sin\varphi_2, \quad (53)$$

$$X_B = X_A - l_4\cos\varphi_4, \quad Y_B = Y_A + l_4\sin\varphi_4, \quad (54)$$

$$X_D = X_A - l_4\cos\varphi_4 - l_5\cos\varphi_5,$$

$$Y_D = Y_A + l_4\sin\varphi_4 + l_5\sin\varphi_5, \quad (55)$$

where X_G, Y_G, X_A, Y_A are constant specified coordinates of the six-link mechanism racks.

The analogs of angular velocities are also defined, which make it possible to determine the linear velocities of the joints of the six-link mechanism.

From the movement of the suspension point D, it can be seen that it is approximately drawing a straight line (Fig. 5).

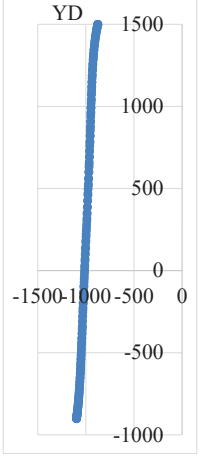

Fig. 5. Suspension point movement

5. 2. Results of the force analysis

As a result of the force analysis, jointly solving the equilibrium equations of the links of the six-link hinge-lever mechanism, the reactions of the hinges of the mechanism were determined (Fig. 4).

Fig. 6 shows the behavior of reactions in the joints of the mechanism C and B, that is, the behavior of the component reactions in the hinge C–RC_x, RC_y, RC_{tau}, RC_{norm}, as well as in the hinge B–RB_x, RB_y, RB_{tau}, RB_{norm}.

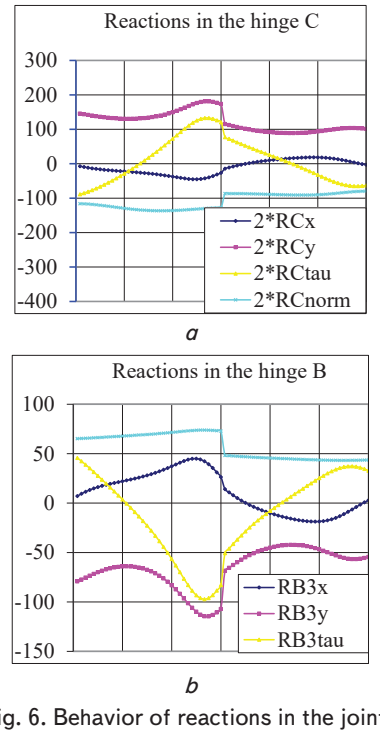

Fig. 6. Behavior of reactions in the joints of the mechanism

6. Discussion of experimental results

The results of the kinematic analysis showed that the connecting rod point D performs an approximately rectilinear movement (Fig. 5), which makes it possible to use this six-link mechanism as a converting mechanism for the SRPD.

Thus, it is possible to eliminate the arc head of the balancer, which leads to a decrease in the metal consumption of the structure.

Also, according to the formulas for determining the angular velocities (41), similarly to (42), we determine the velocities of all hinges and centers of mass of the links of the mechanism, which we will later use to determine the balancing moment according to the d'Alembert principle.

Based on the results of the kinetostatic analysis, graphs of the behavior of the reaction forces in the joints were obtained.

Fig. 6 shows that the tangential components of the reaction forces have alternating signs, which negatively affects the wear of parts elements. This requires further solution of the problem of dynamic synthesis.

Also, to achieve more accurate reproduction of the straight point of suspension of the rod column, we will solve the problem of synthesizing a six-link linkage mechanism to reproduce a vertical straight line.

7. Conclusions

1. A kinematic analysis has been carried out and a mathematical model has been developed for the kinematic analysis of a six-link mechanism in the Maple environment in order to test the performance of the new design.

The obtained numerical results confirm that the suspension point of the rod string makes an approximate rectilinear motion.

2. The reactions in the joints of the six-link mechanism as a converting mechanism were determined. Tangential components of the reactions in the joints were defined.

Acknowledgments

This research has been funded by the Science Committee of the Ministry of Education and Science of the Republic of Kazakhstan (Grant No. AP08052127).

References

1. Torres, L. H. S., Schntman, L. (2013). Sucker-Rod Pumping System of Oil Wells: Modelling, Identification and Process Control. 6th IFAC Conference on Management and Control of Production and Logistics The International Federation of Automatic Control. Fortaleza, 260–265. doi: https://doi.org/10.3182/20130911-3-br-3021.00052
2. Yin, J.-J., Sun, D., Yang, Y. (2020). Predicting multi-tapered sucker-rod pumping systems with the analytical solution. Journal of Petroleum Science and Engineering, 108115. doi: https://doi.org/10.1016/j.petrol.2020.108115
3. Ahmedov, B., Najafov, A., Abdullayev, A. (2018). Determination of the kinematic parameters of the new constructive solution of the beamless sucker-rod pump. Journal of Structural Engineering & Applied Mechanics, 1 (3), 128–135. doi: https://doi.org/10.31462/jseam.2018.03128135
4. Dumitru, N., Baila, A., Craciunoiu, N., Malciu, R. (2011). Dynamic analysis of the oil rod pumping system mechanism. Proceedings of the 22nd International DAAAM Symposium, 22 (1).
5. Kennedy, F. F., Michel, L., Frederic, L., Abbas, N., Njoke, M. (2015). Hands-on model of sucker rod pumping facility for oil well production. Journal of Petroleum and Gas Engineering, 6 (4), 45–53. doi: https://doi.org/10.5897/jpge2015.0220
6. Volokhin, A. V., Volokhin, E. A., Arsibekov, D. V. (2019). Improving the beam-balanced pumping unit. Petroleum Engineering, 17 (5), 114. doi: https://doi.org/10.17122/ngdelo-2019-5-114-122
7. Tan, C., Li, G., Qu, Y., Yan, X., Bangert, P. Predicting the Dynamometer Card of a Rod Pump. Algorithmica Technologies. Available at: http://www.algorithmica-technologies.com/system/case_studies/pdf_ens/000/000/012/original/09_Predicting_the_Dynamometer_Card_of_a_Rod_Pump.pdf?1457398050
8. Singal, K., Zamanian, F., Marotta, E., Sivaramakrishnan, S. (2014). Pat. No. US9605670B2. Method and systems for enhancing flow of a fluid induced by a rod pumping unit. No. 14/575,789; declareted: 18.12.2014; published: 23.06.2016. Available at: https://patentimages.storage.googleapis.com/d0/fc/c6/8d2811fbd0f53c/US9605670.pdf
9. Ibraev, S., Nurmaganbetova, A., Imanbaeva, N., Zhauyt, A. (2017). Computerized modeling of kinematics and kineto-statics of sucker-rod pump power units. Engineering for rural development, 904–909. doi: https://doi.org/10.22616/erdev2017.16.n184
10. Imanbaeva, N. S., Nurmaganbetova, A. T., Isametova, M. E., Rakhmatulina, A. B., Sakenova, A. M. (2017). Study mode converts trim mechanism sucker rod pumping units (SRPU), to determine the distance from the rotational axis of the counterweight crank. Vestnik KazNRTU, 1, 328–332.